biology and life sciences forum

MDPI

Proceeding Paper

Rapid Assessment of Protein Structural Changes from Frost Damage: A Proof-of-Concept Study Using *Pittosporum spinescens* (Apiales) †

Joel B. Johnson

School of Health, Medical & Applied Sciences, Central Queensland University, Bruce Hwy, North Rockhampton, QLD 4701, Australia; joel.johnson@cqumail.com

† Presented at the 2nd International Electronic Conference on Plant Sciences—10th Anniversary of Journal Plants, 1–15 December 2021. Available online: https://iecps2021.sciforum.net/.

Abstract: Frost damage remains an important driver of floral ecological dynamics in certain areas of the Australian landscape. However, responses of native Australian species to frost damage remain largely understudied. Here, attenuated total reflectance Fourier transform infrared (ATR-FTIR) spectroscopy, conducted on intact leaves, was used to monitor changes in the protein secondary structures of *Pittosporum spinescens* upon exposure to below-zero temperatures. The dominant secondary structures present in fresh leaves were the inter-molecular aggregates (40%), α-helices (20%), β-sheets (15%) and random coil structures (14%). During simulated severe frost (−18 °C), a reduction in α-helices and increase in the amount of inter-molecular structures were observed, followed by transmutation of the latter into anti-parallel β-sheets or another form of inter-molecular structures. After 6 h, the dominant protein secondary structures were anti-parallel β-sheets and inter-molecular aggregates (*ca.* 64% and 17%, respectively), with only small amounts of α-helices (4%), β-sheets (9%) and random coil structures (5%) present. Overall, this indicates a reduction in the organisation level of protein secondary structures, resulting in a probable loss of function and considerable damage to the functional activity of any proteins in the leaves. The technique of ATR-FTIR spectroscopy should be considered by future researchers interested in investigating responses to frost damage in other species, particularly at an ecological level. Portable FTIR instrumentation would greatly expand the potential range of applications.

Keywords: fourier transformed infrared (FTIR) spectroscopy; frost resistance; cold tolerance; hardening

Citation: Johnson, J.B. Rapid Assessment of Protein Structural Changes from Frost Damage: A Proof-of-Concept Study Using *Pittosporum spinescens* (Apiales). *Biol. Life Sci. Forum* **2021**, *1*, x. https://doi.org/10.3390/xxxxx

Academic Editor: Ki Hyun Kim

Published: 30 November 2021

1. Introduction

In contrast to the well-known and well-studied effects of fire on the present Australian flora, the role of frost is less publicised [1]. Nevertheless, frost has played an important historical role in influencing the distribution and genotypes of Australian flora [2,3]. Furthermore, some regions of central Tasmania and southern New South Wales still incur frost on over 150 days per year [4], making this an important factor regulating species' contemporary distributions [5].

While several Australian studies have investigated the responses of certain plant species to frost damage, these are primarily restricted to a few species due to the time-consuming methods involved, such as measuring changes in electrical conductivity [6] or chlorophyll fluorescence [7]. Fourier transform infrared (FTIR) spectroscopy is emerging as a rapid analytical technique for gathering information about the sub-molecular characteristics of various matrices, including the secondary structure of proteins (α-helices vs β-sheets), relative proportions of various carbohydrates and lipids, and starch structure (crystalline vs amorphous) of food products. Xin et al. [8] investigated the chemical changes associated with frosted wheat kernels using FTIR spectroscopy, but aside from

this, very little research appears to have been conducted using FTIR to investigate the molecular effects of frost damage on plant tissue.

This proof-of-concept study demonstrates the use of FTIR spectroscopy to probe the changes in protein secondary structure of *Pittosporum spinescens* (F.Muell.) L. Cayzer, Crisp & I. Telford) leaves exposed to below-zero temperatures. This species is principally found on the north- to mid-eastern coast of Australia, with an estimated frost resistance down to temperatures of ca. −6 °C [9].

2. Materials and Methods

2.1. Sample Collection, Treatment and Spectra Acquisition

Intact branches (including leaves) were collected from the northern side of a single *P. spinescens* bush in Central Queensland (23.765°S, 150.351°E) in January 2020, and transported to the laboratory (approximately 10 °C for 1 h). Spectra were collected from the adaxial surfaces of the fresh leaves using a Bruker Alpha FTIR spectrophotometer (Bruker Optics Gmbh, Ettlingen, Germany) with a platinum diamond attenuated total reflectance (ATR) single reflection module (4000–400 cm^{-1}; 4 cm^{-1} resolution; average of 24 scans/spectra). The leaves were subsequently transferred to a freezer (−18 °C), with further spectra collected from the leaves after 15 min, 30 min, 1 h, 3 h and 6 h of freezing. To allow for statistical analysis, spectra were collected from five biological replicates (i.e., different leaves) at each time point.

2.2. Data Analysis

Peak positions were identified using Spectragryph (Friedrich Menges, Oberstdorf, Germany). Peaks were fitted and analysed in PeakFit® v4.12 (Systat Software, San Jose, CA, USA). Statistical tests were performed with IBM SPSS (v25). To analyse the secondary structures of the proteins present in the leaves, the spectral region corresponding to the amide I bond, between 1700–1580 cm^{-1}, was deconvoluted into its constituent peaks using PeakFit®. In order to do this, the region between 1700–1580 cm^{-1} of each spectrum was first fitted with a linear two-point baseline. Following Savitsky-Golay smoothing at 1%, peaks were fitted and quantified using a Gaussian amplitude algorithm with the autoscan algorithm set at 1.5% amplitude. The area under each peak was assumed to be proportional to the amount of the corresponding protein structures, following Suresh et al. [10]. Peak assignments followed relevant literature [11].

3. Results and Discussion

3.1. FTIR Spectra

The averaged FTIR spectra of the fresh *P. spinescens* leaves is shown in Figure 1. The broadest peak, centred at 3345 cm^{-1}, resulting from the OH stretch of water in the sample, while the two sharp peaks at 2915 and 2847 cm^{-1} are from CH_3 symmetric stretch and CH_2 anti-symmetric stretch, respectively [10]. These latter groups are most likely due to the presence of lipids or fatty acids present in the sample. The next major peak was centred at 1605 cm^{-1}, with a shoulder at 1710 cm^{-1}. The former was attributed to the amide I bond of proteins [12], with the latter possibly from the stretch of free keto groups [10], such as those found in triglycerides. The peak at 1515 cm^{-1} appears to be from N-H bend and C-N stretch of the Amide II bond, although present at a slightly lower wavenumber than that typically reported previously [10]. Similarly, the peak at 1261 cm^{-1} was attributed to the Amide III band of proteins. Absorbance at 1460 cm^{-1} is attributed to the O-H bend of cellulose, while the peak at 1368 cm^{-1} is likely from CH_2 symmetric bending, although CH_3 bend could also have some contribution [12].

The dual peak present at around 1200 and 1171 cm^{-1} likely resulting from a combination of pectin, ester groups or phenolic compounds [12]. Absorbance from C-O bend and C-O stretch also occurs in this region. The peak at 1068 cm^{-1} is attributed to a combination band of various bonds present in cellulose, including C-O and C-C stretch, and C-O-H

bend [12]. The right-most shoulder of this peak, approaching 1000 cm^{-1}, could result from starch and/or other structural carbohydrates [13]. Finally, the small peak at 720 cm^{-1} could result from the C-H bend, C-O stretch or C-C stretch of structural carbohydrates [14].

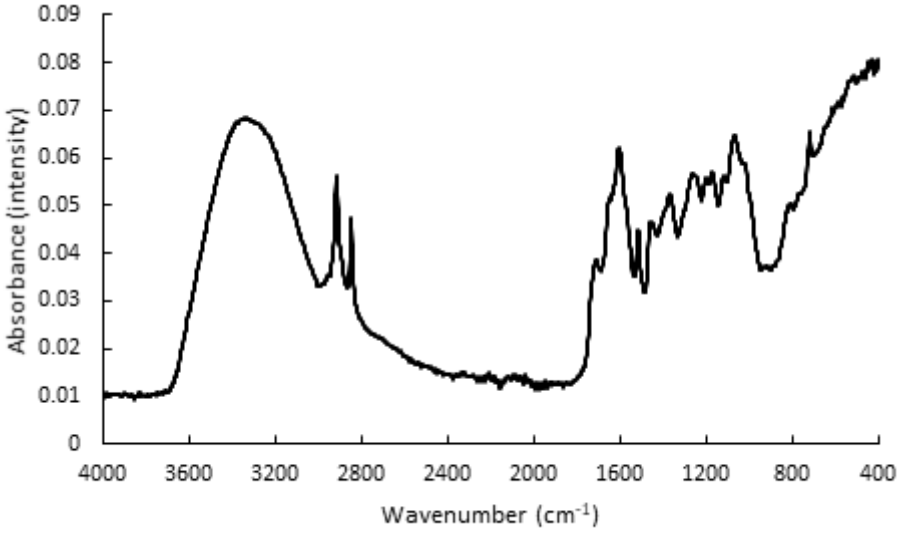

Figure 1. Averaged FTIR spectra taken from the adaxial side of five *Pittosporum spinescens* leaves.

3.2. Protein Secondary Structure

Frost damage primarily results from physical cellular damage, following the nucleation of water into ice crystals which compromises the integrity of the cell wall structure [15]. An important secondary impact of damage is the disruption of key functional proteins, either through ice crystal formation physically breaking the proteins apart, or through water crystallisation disrupting intra- and inter-molecular bonding, which depend highly on the presence of water molecules to stabilise hydrogen bonds. In turn, this disrupts the tertiary structure and the overall functioning of the protein, mediating the physiological damage that results from frost, even if the cell membrane remains intact [16]. Additionally, certain proteins have been implicated as contributors toward the frost resistance of tolerant species [17], which may be detectable through FTIR spectroscopy. Given the key role that proteins appear to play in mediating frost damage, the primary focus of this study was on the changes in protein structure associated with frost damage.

Alterations in protein secondary structures have been noted during the thawing and freezing of red meat (Sun et al. 2016). Similarly, Xin et al. [8] observed that frosted wheat kernels had lower levels of amide bonds and a lower ratio of amide I: II, but no significant differences in the ratios of α-helices to β-sheets.

In the fresh leaves, the dominant protein secondary structures present were the inter-molecular aggregates (40%), followed by α-helices (20%), β-sheets (15%) and random coil (14 %) (Table 1). Peaks below 1609 cm^{-1} were tentatively assigned to anti-parallel β-sheets [18], due to lack of literature references available on secondary protein structures causing absorbance at these wavenumbers. However, it is also possible that these peaks could result from different forms of inter-molecular aggregates, particularly at the higher wavenumbers (e.g., 1602 cm^{-1}). The predominant protein present in fresh *P. spinescens* leaves is likely to be rubisco (ribulose-1,5-bisphosphate carboxylase/oxygenase), the enzyme which captures CO_2 in the first major stage of C_3 photosynthesis. In addition to the potential disruption of other portions of the photosynthetic pathway, loss of rubisco functionality would concur with the observed effects of frost damage resulting in a loss of photosynthetic activity [9].

Table 1. Relative amounts of protein secondary structures identified in the *Pittosporum spinescens* leaves. Data is given as percentage of the total protein structures identified, measured according to the area under the spectral curve. Where a significant difference between timepoints was found, timepoints with the same subscript letter were not significantly different to each other at $\alpha = 0.05$.

Peak Centre	Protein Structure	Length of Simulated Frost (hrs)						*p* Value
		0	0.25	0.5	1	3	6	
1589 cm^{-1}	Anti-parallel β-sheet ^/	0 ^{a}	0 ^{a}	0 ^{a}	0 ^{a}	0 ^{a}	4.0 ^{b}	**0.002**
1594 cm^{-1}	inter-molecular aggre-	10.3	8.5	11.0	12.5	7.4	6.6	0.648
1602 cm^{-1}	gates	0 ^{a}	11.6 ^{a}	0 ^{a}	0.7 ^{a}	0 ^{a}	53.7 ^{b}	**<0.001**
Sum	″	10.3 ^{a}	20.1 ^{a}	11.0 ^{a}	13.2 ^{a}	7.4 ^{a}	64.3 ^{b}	**<0.001**
1609 cm^{-1}	Inter-molecular aggre-	32.6 ^{a,b,c}	13.9 ^{a,b}	50.1 ^{c}	35.4 ^{a,b,c}	45.6 ^{b,c}	8.1 ^{a}	**0.003**
1619 cm^{-1}	gates	6.9	23.3	6.7	9.7	1.5	8.4	0.110
Sum	″	39.5 ^{a,b}	37.2 ^{a,b}	56.8 ^{b}	45.1 ^{a,b}	47.1 ^{b}	16.5 ^{a}	**0.009**
1629 cm^{-1}	β-sheets	0	10.7	3.1	7.3	0	4.0	0.168
1635 cm^{-1}		15.2	16.6	5.9	9.1	16.5	5.3	0.162
Sum	″	15.2	27.3	9.0	16.4	16.5	9.3	0.196
1648 cm^{-1}	Random coils	14.3	8.2	5.4	14.2	22.6	4.6	0.062
1653 cm^{-1}	α-helices	19.6 ^{a}	7.4 ^{a}	17.5 ^{a}	10.4 ^{a}	4.9 ^{a}	4.4 ^{a}	**0.035**
1662 cm^{-1}	3_{10} helix	0.4	0	0	1.1	0.8	0.5	0.706
1667 cm^{-1}	β-turn	0.7	0	0.2	0	0.7	0.4	0.662
		Peak heights						
1653 cm^{-1}	α-helices	0.0508 ^{b}	0.0299 ^{a}	0.0508 ^{b}	0.0537 ^{b}	0.0808 ^{c}	0.0409 ^{a,b}	**<0.001**
1635 cm^{-1}	β-sheets	0.0526 ^{b}	0.0313 ^{a}	0.0495 ^{b}	0.0587 ^{b}	0.0860 ^{c}	0.0438 ^{a,b}	**<0.001**
Ratio	α-helices: β-sheets	0.968 ^{b}	0.954 ^{a,b}	1.022 ^{c}	0.916 ^{a}	0.939 ^{a,b}	0.935 ^{a,b}	**<0.001**

^ potential assignment.

With increasing periods of freezing (Table 1), there was no significant change in the relative proportion of β-sheet structures present, but a significant reduction in the relative proportion of α-helices were observed ($p = 0.009$). This resulted in a significant alteration to the ratio of α-helices: β-sheets ($p < 0.001$). Many of the other changes in the relative proportions of protein structures were not statistically significant. However, the level of inter-molecular aggregates (as measured at 1609 cm^{-1}) increased up until 3 h of freezing. Between 3 and 6 h, these inter-molecular aggregates appeared to be converted to another form with a peak absorbance at 1602 cm^{-1}, apparently comprising anti-parallel β-sheets or a different form of inter-molecular aggregates. This created a marked rise in the contribution of the 1602 cm^{-1} peak at the 6-h timepoint. In addition, the formation of a peak at 1589 cm^{-1} occurred at the 6-h timepoint. This could be attributed to the anti-parallel β-sheets already present in the samples, but with altered absorption characteristics resulting from slippage in the relative position of the residues [18].

Overall, freezing appeared to particularly interfere with the sub-molecular structural organisation level of α-helices, which rely on the presence of free water molecules to maintain structural integrity via hydrogen bonding [19]. These (along with small amounts of other secondary structures) were apparently converted into inter-molecular aggregates. After greater than 3 h of exposure to freezing temperatures, these inter-molecular aggregates continue to change form, resulting in the formation of a protein structure not observed at any point prior. Although further work would be necessary to determine the key proteins being affected, the overall loss of protein structure and function is likely to be one of the major contributing factors in the physiological damage pathway.

Although the FTIR spectroscopy apparatus used in this study was a benchtop system, portable FTIR instrumentation, such as the Agilent 4300 Handheld FTIR, could potentially be useful for real-time analysis of plant samples in the field. This could allow for the non-destructive, in-field assessment of leaf samples while still attached to the plant,

saving significant amounts of time. This may also allow for the analysis of frost resistance/damage at an ecosystem level. The protein structural composition in the leaves of various species could be determined during the daytime, with subsequent analysis on the same species following (or even during) a frost event. This would provide far greater insight into the diversity and complexity of physiological responses and frost-driven population dynamics in the ecosystem being explored. Other studies could explore differences in frost damage responses associated with ecological niches or certain genotypes. It is also possible that FTIR spectroscopy could be used to provide information on the physiological responses of flora to other stressors, such as extreme temperatures or drought stress. The cost of this instrumentation is continuing to fall, making this an area for interested readers to watch closely.

Frost damage is also of prime interest from an economic perspective, accounting for a significant proportion of crops grown for both human consumption [20] and fodder [21], particularly in the Northern Hemisphere. For this reason, the bio- and macro-chemical profiling and development of frost-resistance varieties has been a high priority for breeding programmes of crops [22] and fodder [23,24]. The technique of FTIR spectroscopy, used here to gain insight into the response of a native plant species to frost damage, could be extended to commercial crops, with the view of providing detailed information about the physiochemical responses to frost damage. The information gathered could prove useful for comparing frost resistance between various genotypes of the same species or for screening purposes in breeding trials. Again, very little FTIR work has been conducted in this area, so proof-of-concept studies followed by validation studies on commercial crops are sure to be welcomed by the plant breeding community.

4. Conclusions

ATR-FTIR spectroscopy was applied for the analysis of protein secondary structures in intact *Pittosporum spinescens* leaves. This technique confirmed that exposure to temperatures well below 0 °C caused a reduction in organised protein structures, particularly α-helices, while causing an increase in the level of disorganised, inter-molecular aggregates. This loss of protein function is thus one significant mechanism behind the physiology of frost damage. ATR-FTIR spectroscopy is likely to be of interest to future researchers investigating responses to frost damage, in both the natural and agricultural ecosystems.

Funding: This research received no external funding.

Data Availability Statement: The data presented in this study are available on request from the corresponding author.

Conflicts of Interest: The author declares no conflict of interest.

References

1. Inouye, D.W. The ecological and evolutionary significance of frost in the context of climate change. *Ecol. Lett.* **2000**, *3*, 457–463. https://doi.org/10.1046/j.1461-0248.2000.00165.x.
2. Busby, J.R. A biogeoclimatic analysis of Nothofagus cunninghamii (Hook.) Oerst. in southeastern Australia. *Aust. J. Ecol.* **1986**, *11*, 1–7.
3. Barnes, R.W.; Hill, R.S.; Bradford, J.C. The history of Cunoniaceae in Australia from macrofossil evidence. *Aust. J. Bot.* **2001**, *49*, 301–320. https://doi.org/10.1071/BT00036.
4. Bureau of Meteorology. Annual and Monthly Potential Frost Days. Available online: http://www.bom.gov.au/jsp/ncc/climate_averages/frost/index.jsp (accessed on Jan 21).
5. Blake, J.; Hill, R. An Examination of the Drought and Frost Tolerance of *Banksia marginata* (Proteaceae) as an Explanation of Its Current Widespread Occurrence in Tasmania. *Aust. J. Bot.* **1996**, *44*, 265–281. https://doi.org/10.1071/BT9960265.
6. Raymond, C.; Harwood, C.; Owen, J. A Conductivity Method for Screening Populations of Eucalypts for Frost Damage and Frost Tolerance. *Aust. J. Bot.* **1986**, *34*, 377–393. https://doi.org/10.1071/BT9860377.
7. Percival, G.; Henderson, A. An assessment of the freezing tolerance of urban trees using chlorophyll fluorescence. *J. Hortic. Sci. Biotechnol.* **2003**, *78*, 254–260.
8. Xin, H.; Zhang, X.; Yu, P. Using synchrotron radiation-based infrared microspectroscopy to reveal microchemical structure characterization: Frost damaged wheat vs. normal wheat. *Int. J. Mol. Sci.* **2013**, *14*, 16706–16718.

9. Stuart, S.A. Cold Comfort: Diversification and Adaptive Evolution across Latitudinal Gradients. Ph.D. Thesis, University of California, Berkeley, Berkeley, CA, USA, 2011.
10. Suresh, S.; Karthikeyan, S.; Jayamoorthy, K. FTIR and multivariate analysis to study the effect of bulk and nano copper oxide on peanut plant leaves. *J. Sci. Adv. Mater. Devices* **2016**, *1*, 343–350. https://doi.org/10.1016/j.jsamd.2016.08.004.
11. Kong, J.; Yu, S. Fourier transform infrared spectroscopic analysis of protein secondary structures. *Acta Biochim. Biophys. Sin.* **2007**, *39*, 549–559.
12. Moskal, P.; Wesełucha-Birczyńska, A.; Łabanowska, M.; Filek, M. Adaxial and abaxial pattern of Urtica dioica leaves analyzed by 2DCOS ATR-FTIR as a function of their growth time and impact of environmental pollution. *Vib. Spectrosc.* **2019**, *104*, 102948. https://doi.org/10.1016/j.vibspec.2019.102948.
13. Capron, I.; Robert, P.; Colonna, P.; Brogly, M.; Planchot, V. Starch in rubbery and glassy states by FTIR spectroscopy. *Carbohydr. Polym.* **2007**, *68*, 249–259.
14. Chen, Y.; Cao, X.; Chang, P.R.; Huneault, M.A. Comparative study on the films of poly (vinyl alcohol)/pea starch nanocrystals and poly (vinyl alcohol)/native pea starch. *Carbohydr. Polym.* **2008**, *73*, 8–17.
15. Sutinen, M.-L.; Arora, R.; Wisniewski, M.; Ashworth, E.; Strimbeck, R.; Palta, J. Mechanisms of frost survival and freeze-damage in nature. In *Conifer Cold Hardiness*; Springer: Berlin/Heidelberg, Germany, 2001; pp. 89–120.
16. Mayland, H.; Cary, J. Frost and chilling injury to growing plants. *Adv. Agron.* **1970**, *22*, 203–234.
17. Kacperska-Palacz, A.; Dlugokecka, E.; Breitenwald, J.; Wciślińska, B. Physiological mechanisms of frost tolerance: Possible role of protein in plant adaptation to cold. *Biol. Plant.* **1977**, *19*, 10–17.
18. Hiramatsu, H.; Kitagawa, T. FT-IR approaches on amyloid fibril structure. *Biochim. Biophys. Acta (BBA)-Proteins Proteom.* **2005**, *1753*, 100–107. https://doi.org/10.1016/j.bbapap.2005.07.008.
19. Sundaralingam, M.; Sekharudu, Y. Water-inserted alpha-helical segments implicate reverse turns as folding intermediates. *Science* **1989**, *244*, 1333–1337.
20. Reingold, N. *Cold Weather Agriculture*; Science and Technology Division, Library of Congress: 1960.
21. Thorsen, S.M.; Höglind, M. Assessing winter survival of forage grasses in Norway under future climate scenarios by simulating potential frost tolerance in combination with simple agroclimatic indices. *Agric. For. Meteorol.* **2010**, *150*, 1272–1282.
22. Maqbool, A.; Shafiq, S.; Lake, L. Radiant frost tolerance in pulse crops—A review. *Euphytica* **2010**, *172*, 1–12.
23. Junttila, O.; Svenning, M.M.; Solheim, B. Effects of temperature and photoperiod on frost resistance of white clover (Trifolium repens) ecotypes. *Physiol. Plant.* **1990**, *79*, 435–438.
24. Rognli, O.A. Breeding for improved winter survival in forage grasses. In *Plant and Microbe Adaptations to Cold in a Changing World*; Springer: Berlin/Heidelberg, Germany, 2013; pp. 197–208.